Experimental evolution of multicellularity

William C. Ratcliff[a,1], R. Ford Denison[a], Mark Borrello[a], and Michael Travisano[a,b]

[a]Department of Ecology, Evolution and Behavior and [b]BioTechnology Institute, University of Minnesota, Minneapolis, MN 55108

Edited* by Richard E. Lenski, Michigan State University, East Lansing, MI, and approved December 14, 2011 (received for review September 19, 2011)

Multicellularity was one of the most significant innovations in the history of life, but its initial evolution remains poorly understood. Using experimental evolution, we show that key steps in this transition could have occurred quickly. We subjected the unicellular yeast *Saccharomyces cerevisiae* to an environment in which we expected multicellularity to be adaptive. We observed the rapid evolution of clustering genotypes that display a novel multicellular life history characterized by reproduction via multicellular propagules, a juvenile phase, and determinate growth. The multicellular clusters are uniclonal, minimizing within-cluster genetic conflicts of interest. Simple among-cell division of labor rapidly evolved. Early multicellular strains were composed of physiologically similar cells, but these subsequently evolved higher rates of programmed cell death (apoptosis), an adaptation that increases propagule production. These results show that key aspects of multicellular complexity, a subject of central importance to biology, can readily evolve from unicellular eukaryotes.

complexity | cooperation | major transitions | individuality | macro evolution

The evolution of multicellularity was transformative for life on earth (1). In addition to larger size, multicellularity increased biological complexity through the formation of new biological structures. For example, multicellular organisms have evolved sophisticated, higher-level functionality via cooperation among component cells with complementary behaviors (2, 3). However, dissolution and death of multicellular individuals occurs when cooperation breaks down, cancer being a prime example (4). There are multiple mechanisms to help ensure cooperation of component cells in most extant multicellular species (5–8), but the origin and the maintenance of multicellularity are two distinct evolutionary problems. Component cells in a nascent multicellular organism would appear to have frequent opportunities to pursue noncooperative reproductive strategies at a cost to the reproduction of the multicellular individual. How, then, does the transition to multicellularity occur?

Understanding the evolution of complex multicellular individuals from unicellular ancestors has been extremely challenging, largely because the first steps in this process occurred in the deep past (>200 million years ago) (9, 10). As a result, transitional forms have been lost to extinction, and little is known about the physiology, ecology, and evolutionary processes of incipient multicellularity (11). Nonetheless, several key steps have been identified for this transition. Because multicellular organisms are composed of multiple cells, the first step in this transition was likely the evolution of genotypes that form simple cellular clusters (1, 3, 12–16). It is not known whether this occurs more readily although aggregation of genetically distinct cells, as in biofilms, or by mother–daughter cell adhesion after division. Once simple clusters have evolved, selection among multicelled clusters must predominate over selection among single cells within clusters (1, 15, 17, 18). The mode of cluster formation may affect the occurrence of this shift. Aggregation of genetically distinct free-living cells could lead to conflicts of interest among cells within the cluster, potentially inhibiting adaptation in cluster-level traits (6, 19, 20). Clusters that are formed via postdivision adhesion are uniclonal and thus avoid this potential conflict. Finally, for cellular differentiation to evolve, division of labor among cells within a cluster must increase cluster-level fitness (15, 21–23).

Prior experimental work with de novo transitions to multicellularity have focused mainly on the ecological conditions that would favor the evolution of cellular clusters. Boraas et al. (16) have shown that predation by a small-mouthed ciliate results in the evolution of eight-celled clusters of the previously single-celled algae *Chlorella*. Koschwanez et al. (18) have shown that metabolic cooperation among cluster-forming yeast allows them to grow at low densities prohibitive to growth of single-celled yeast. However, previous work has not systematically examined the de novo evolution of cellular clusters and their subsequent multicellular evolution. Here we use experimental evolution to directly explore the evolution of early multicellularity, focusing on the mode of cluster formation (postdivision adhesion vs. aggregation), the shift from single-cell to cluster-level selection, and the evolution of among-cell division of labor.

We used gravity to select for primitive multicellularity in the unicellular yeast *Saccharomyces cerevisiae*. Clusters of cells settle through liquid more quickly than do single cells, allowing us to easily select for clustering genotypes. Settling selection was chosen not because it is widespread in nature, but rather because it is an experimentally tractable method to select for larger size. Ten replicate populations of initially isogenic *S. cerevisiae* were grown in nutrient-rich liquid medium with shaking to stationary phase (~10^9 cells/replicate population) before subculturing and daily transfer to fresh medium. All replicate populations were allowed to stand for 45 min before transfer to 10 mL fresh medium, during which time cells settled toward the bottom of the culture tube. Cells in the lower 100 μL were then transferred to fresh medium. After the first week, we modified the settling step to be more time efficient by using 100 × *g*, 10-s centrifugations of 1.5-mL subsamples from the shaken 10-mL tube to settle population fractions for transfer to fresh medium. We expected these conditions to select for clusters of cells, whether by postdivision adhesion or by aggregation.

Results

We observed rapid increases in settling rate over the course of selection. After 60 transfers, all populations were dominated by roughly spherical snowflake-like phenotypes consisting of multiple attached cells (Fig. 1 and Figs. S1 and S2). We verified the selective benefit of the snowflake phenotype, showing that it has a 34% fitness advantage over individual cells under the selection conditions (Fig. 2*A*; $t_9 = 4.53$, $P = 0.004$, one-sided *t* test), whereas it appears to suffer a 10% fitness cost in the absence of settling selection ($t_9 = 1.92$, $P = 0.06$, one-sided *t* test).

Author contributions: W.C.R., R.F.D., and M.T. designed research; W.C.R. performed research; W.C.R., R.F.D., M.B., and M.T. analyzed data; and W.C.R., R.F.D., M.B., and M.T. wrote the paper.

The authors declare no conflict of interest.

*This Direct Submission article had a prearranged editor.

Freely available online through the PNAS open access option.

[1]To whom correspondence should be addressed. E-mail: ratcl009@umn.edu.

This article contains supporting information online at www.pnas.org/lookup/suppl/doi:10.1073/pnas.1115323109/-/DCSupplemental.

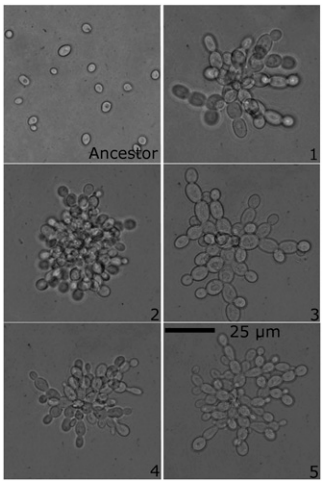

Fig. 1. Rapid and convergent evolution of the multicellular "snowflake" phenotype. All 10 replicate populations (replicate population number in lower right corner) evolved similar multicellular phenotypes after 60 rounds of selection for rapid settling (shown are replicate populations 1–5; see Fig. S2 for replicate populations 6–10). These genotypes display a similar growth form: the cluster is composed of related cells that do not disassociate after budding, resulting in branched multicellularity.

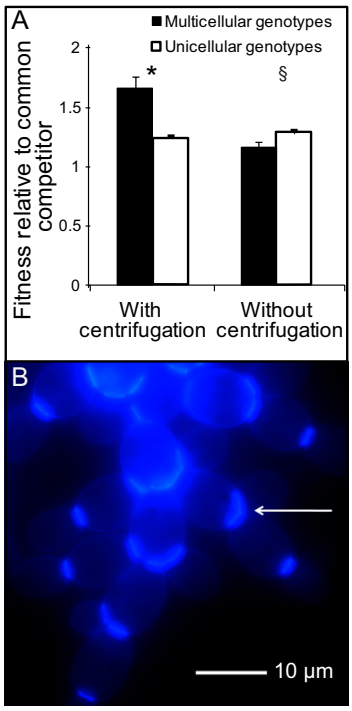

Fig. 2. Evolution of clustering in snowflake-phenotype yeast. (*A*) Clusters have greater fitness only with gravitational selection. Five replicate populations of *S. cerevisiae* strain Y55 were transferred 60 times either with or without selection for settling. One representative genotype was isolated from each population (multicellular cluster with centrifugation, unicellular without centrifugation). The relative fitness of these isolates was determined by competition with a common unicellular competitor and a GFP-marked Y55 isolate either with or without gravitational selection. Relative fitness during a single 24-h growth period (one transfer) was calculated as the ratio of the Malthusian growth parameters of the test strain to the common competitor. Clustering genotypes possess a large fitness advantage with gravitational selection, but appear to pay a small cost when transferred without centrifugation. Significance: $^{*}P = 0.004$, $^{\S}P = 0.06$, one-sided *t* tests. Error bars are the SEM of five replicate populations. (*B*) A representative genotype (drawn from replicate population 1, day 30, of our first evolution experiment) was grown overnight in yeast peptone dextrose (YPD) media and stained with the blue-fluorescent chitin-binding fluorescent stain calcofluor. All attachments between cells occur at "bud scars" (arrow), demonstrating that the cluster is formed by incomplete separation of daughter and mother cells.

Mechanism of Cluster Formation. In theory, multicellular clusters could increase in cell number either by aggregation of single cells or by postdivision adhesion. The latter method results in high genetic identity within clusters, reducing potential conflict between unicellular and multicellular levels of selection (6, 24). Many genotypes of *S. cerevisiae* aggregate into biofilm-like clusters of cells, termed "flocs," by producing adhesive glycoproteins in their cell walls (25), but we found that snowflake-phenotype yeast do not arise from floc-type aggregation. Individual cells, obtained by enzymatic digestion of snowflake clusters, were tracked via microscopy for 16 h of growth (Movie S1). During this time each cell was seen to give rise to a new snowflake-type cluster, whereas aggregation was never seen, demonstrating that clusters arise via postdivision adhesion and not by aggregation of previously separate cells. Cell adhesion sites were identified by calcofluor staining, which preferentially stains yeast bud scars, confirming that the group of cells making up the snowflake phenotype arises via successive divisions of component cells (Fig. 2*B*). Snowflake yeast are also phenotypically stable: we transferred three replicate populations of snowflake yeast (drawn from replicate population 1, day 30, of our first evolution experiment) 35 times without gravitational selection and did not detect invasion by any unicellular strains.

The snowflake clusters are distinct from *S. cerevisiae* pseudohyphal phenotypes, which have filamentous elongate cells and arise under conditions of nutrient stress (26). Clustering in snowflake-phenotype yeast is independent of pseudohyphal growth, as the snowflake phenotype is stable under both high- and low-nutrient conditions. Individual cells within clusters retain the ancestral ability to form pseudohyphae when starved, but remain oval (not elongate) during standard culture conditions (Fig. S3).

Selection of Multicellular Traits. The evolution of multicellularity requires an increasing role for natural selection among multicellular individuals, relative to selection among cells within individuals (1, 3, 15, 17, 27, 28). We investigated the transition between unicellular and multicellular life by studying two emergent traits of multicellular snowflake-phenotype yeast, cluster reproduction, and settling survival. New clusters can potentially arise by production of either unicellular or multicellular propagules. Examples of both modes of reproduction occur among extant multicellular species, including plants; propagules that develop from a single cell are common among animals (6). We determined the reproductive mode using time-lapse microscopy. Individual clusters were inoculated into 0.5-μL drops of fresh medium and grown overnight. In all cases, daughter clusters (with similar "snowflake" morphology) were produced as multicellular propagules (Fig. 3*A* and Movie S2). These propagules were released sequentially and not via mass dissolution of the parental cluster. In contrast to the unicellular ancestor, which divides into two daughter cells of similar size, propagules were consistently less than half the size of their parental clusters (Fig. 3*B*). No propagules were produced by clusters less than a minimal size, demonstrating that the snowflake phenotype exhibits juvenile/adult life stage differentiation (Fig. 3*B*).

To test for a shift in selection from cell to cluster-level traits, we imposed further selection over 35 transfers, with three contrasting regimes. Conditions were similar to previous experiments, except that we established a gradient in the strength of selection by varying the time available for gravitational settling (5, 15, or 25 min at $1 \times g$) before transfer to fresh medium. The source for the nine new populations, three replicate populations per treatment, was

a single day 30 population in which the snowflake phenotype had already evolved. With mutation as the only source of within-cluster genetic variants, selection among clusters was expected to dominate within-cluster selection, leading to adaptation in multicellular traits. After 35 daily transfers, stronger selection led to greater settling speed. Populations selected under the 5-min regime had a 20% greater settling rate than those populations selected under 15- or 25-min settling schemes (Fig. 3*D*; $F_{2,6} = 15.75$; ANOVA, pairwise differences assessed with Tukey's HSD with $\alpha = 0.05$). Major changes in cluster-level traits that affect settling speed were observed. In the treatment selected for rapid settling, clusters were larger, contained more cells, and produced larger propagules (Fig. 3*C* and Movie S3). Clusters also grew to a similar size and then grew no larger, indicating determinate growth (Fig. 3*C* and Fig. S4). The average size of a cluster at reproduction increased by more than twofold in the 5-min settling treatment, relative to the ancestral snowflake-phenotype cluster before the 35 additional cycles of selection (Fig. 3*E*; $F_{2,119} = 74.5$; $P < 0.0001$; ANOVA, pairwise differences assessed with Tukey's HSD with $\alpha = 0.05$). The longer juvenile phase, which delays propagule production until the parental cluster is larger (Fig. 3*C*), is an emergent multicellular trait. Because the response to selection changed the multicellular phenotype, we conclude that selection was acting on the reproduction and survival of individual clusters rather than on that of their component cells.

Within-Cluster Division of Labor. Cellular differentiation is a hallmark of complex multicellularity. However, the conditions required for its evolution are stringent, particularly when one cell type sacrifices direct reproduction to benefit the whole. Cells that forgo reproduction must be related to those that reproduce [i.e., positive Hamilton's r (24)], and benefits of divided labor must exceed the opportunity cost of lost reproduction (21). We observed the evolution of division of labor through programmed cell death (apoptosis), a mechanism used by snowflake yeast to increase propagule number at the expense of propagule size.

Optimal propagule size depends on a trade-off between the settling rate and the relative growth rate of snowflake yeast. Large-bodied, fast-settling snowflake yeast grow less quickly than smaller snowflake yeast, possibly because interior cells become resource limited in large clusters (Fig. 4*A*; $F_{1,10.8} = 9.89$; $P = 0.0094$; REML-ANCOVA, adjusted $r^2 = 0.52$). For rapid-settling snowflake yeast with slow growth rates, this trade-off may be mitigated by the production of smaller propagules (relative to the cluster producing them). Snowflake yeast that produce smaller propagules can make more of them, increasing a cluster's fecundity, and smaller propagules will be relatively faster growing than larger propagules (Fig. 4*A*). To generate proportionally smaller propagules, each reproductive event must be asymmetric, with propagules having less than half the biomass of the parent. Apoptotic cells may generate "weak links" that allow small branches to separate from large clusters (Fig. S5), resulting in the production of relatively smaller propagules.

In the first multicelled genotypes to evolve (14–28 transfers), the frequency of apoptotic cells [determined by dihydrorhodamine 123 (DHR) staining of reactive oxygen species (29–31)] was not correlated with settling rate (Fig. 4*B*; $P = 0.91$; $r^2 = 0.005$ linear regression). Therefore, apoptosis is not simply a side effect of

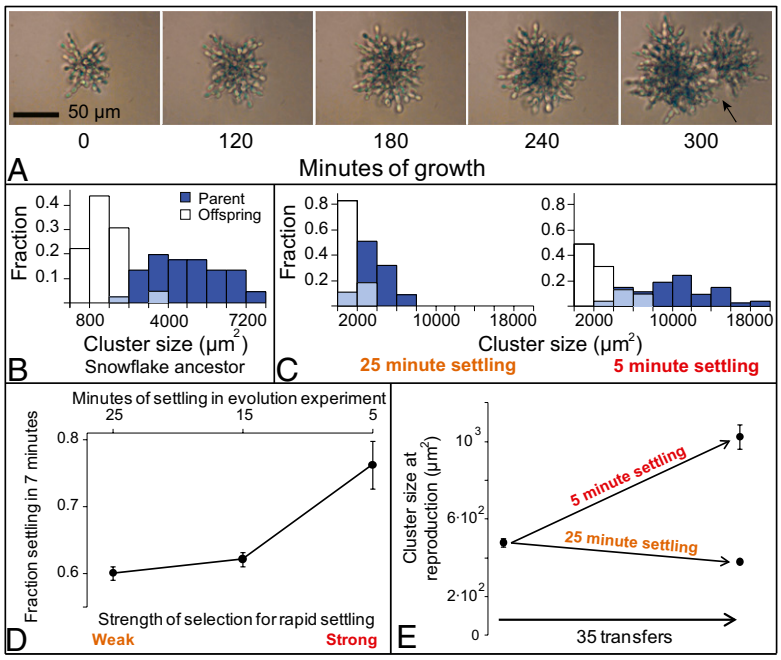

Fig. 3. Snowflake-phenotype yeast have a novel multicellular life history that responds to selection. (*A*) Time-lapse microscopy of a small cluster shows that 300 min of growth and numerous cell divisions are required before the cluster first reproduces (arrow points to propagule separation). Small clusters are thus functionally juvenile, requiring further growth before becoming reproductively competent. (*B*) Analysis of cluster size at reproduction (dark blue bars) and offspring size (open bars, overlap shown in light blue) for the same genotype demonstrates that propagules nearly always start out functionally juvenile. (*D*) A single population of snowflake yeast was exposed to divergent selection for settling rate by allowing yeast to settle for either 5, 15, or 25 min at $1 \times g$ before transfer. A shorter period before transfer imposes stronger selection for rapid settling. After 35 transfers, settling rate was assayed by examining the fraction of yeast biomass in the lower 30% of the culture after 7 min of settling at $1 \times g$. Populations transferred with strong selection for settling (5 min) evolved to settle more rapidly than populations exposed to weaker selection for rapid settling (15 and 25 min). Error bars are the SEM of three replicate populations. (*C* and *E*) The adaptations that resulted in the evolution of faster settling occurred as a result of a change in the cluster-level, not in unicellular life history. Populations selected for more rapid settling (5 min) evolved to delay reproduction until they reached a significantly larger size than the ancestral genotype, whereas relaxed selection for rapid settling resulted in the evolution of clusters that reproduced at a smaller size than the ancestor. Error bars are the SEM of a randomly selected genotype from the population.

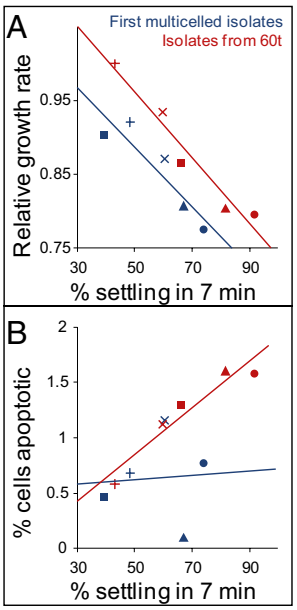

Fig. 4. Across-population comparison of early vs. late snowflake phenotype yeast. (*A*) Snowflake-phenotype yeast face a trade-off between growth and settling rates. Relative growth rate is calculated as the number of doublings per isolate during a 4-h experiment, relative to the fastest growing isolate. Snowflake yeast adapted during the course of the experiment, moving the trade-off function away from the origin. Symbols indicate the replicate population (▲, replicate population 1; ■, replicate population 5; ✕, replicate population 7; ●, replicate population 8; + replicate population 9). (*B*) The frequency of apoptotic cells (measured by dihydrorhodamine 123 staining for reactive oxygen species) was not correlated with settling rate in the first snowflake genotypes to evolve in each population ($r^2 = 0.005$). By 60 transfers, however, settling rate and apoptosis are highly correlated ($r^2 = 0.91$).

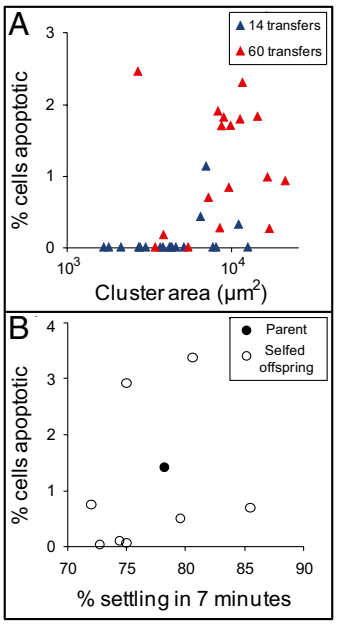

Fig. 5. Apoptosis is not a side effect of large cluster size. (*A*) We measured the relationship between the size of individual clusters and the percentage of cells that were apoptotic. Among clusters of a single genotype (isolated from either 14 or 60 transfers), there was no measurable effect of cluster size on apoptosis frequency ($P = 0.36$, ANCOVA with yeast strain as the cofactor) among snowflake yeast isolated after either 14 or 60 transfers from replicate population 1. (*B*) To determine if cluster size and apoptosis frequency are independently heritable, we selfed an isolate that forms large clusters with high rates of apoptosis and then assayed the resulting fast-settling progeny for apoptosis. Again, there was no relationship between cluster size (measured by settling rate) and apoptosis frequency ($P = 0.55$, linear regression). These results demonstrate that apoptosis is not simply a side effect of large cluster size, but rather that isolates evolving larger cluster size also evolved higher rates of apoptosis.

snowflake size. After further selection (60 transfers total), however, the frequency of apoptotic cells within snowflake clusters was highly correlated with settling rate (Fig. 4*B*; $P = 0.01$; $r^2 = 0.91$, linear regression). To test the hypothesis that large cluster size favors the evolution of apoptosis, rather than causing it directly, we performed two additional experiments. In contrast to correlations across genotypes (Fig. 4*B*), we found no relationship within a genotype between the size of an individual cluster and the fraction of apoptotic cells (Fig. 5*A*). Next, we put an isolate that forms large clusters and exhibits high rates of apoptosis through one round of selfing sex and then examined settling rate and apoptosis in the resulting offspring. Again, these traits were not correlated (Fig. 5*B*), demonstrating that that apoptosis is not simply a side effect of large cluster size. Large average cluster size and higher rates of apoptosis have apparently coevolved.

Dead cells were often stunted or otherwise morphologically aberrant (Fig. S6), potentially decreasing the strength of their connection to daughter cells. With short-term time-lapse microscopy, we have observed propagule separation occurring between a pair of dead cells using video microscopy (Movie S4). To determine whether dead cells are generally involved in propagule separation, we examined their location within propagules. Because clusters grow through parent–offspring adhesion, the central (oldest) cell in the propagule is the site of separation from the parent cluster. The frequency of death in these central cells (76%) was far in excess of the random expectation (6%; $P < 0.0001$, $n = 17$, binomial probability test) in individuals with one or more dead cells, demonstrating an association between cell death and separation of propagules from parents. Manual fragmentation of snowflake clusters did not cause cell death (Fig. S7), so dead cells in propagules are more likely to be a cause than a consequence of cell separation.

To further test the hypothesis that apoptosis is a cause of propagule separation, and not its consequence, we compared size at reproduction and percentage apoptosis in isolates drawn from 14- and 60-transfer populations. We also experimentally induced increased apoptosis and observed its effects on propagule size. After 14 transfers, snowflake phenotype yeast have only the low ancestral rates of apoptosis (Fig. 6*A*) and propagules that are 40% the size of their parents (Fig. 6*D*), whereas 60-transfer isolates have more apoptosis (Fig. 6*B*) and propagules that are less than 20% the size of parent clusters (Fig. 6*D*; $F_{1,20} = 15.72$, $P = 0.002$, Bonferroni-corrected preplanned contrast). Proportionally smaller propagules resulted from a large increase in parent size and only a small increase in propagule size. From transfer 14 to 60, cluster size at reproduction increased from an average of 3,042–9,075 μm^2, and offspring size increased from an average of 1,193–1,871 μm^2. To test the hypothesis that apoptosis results in the production of proportionally smaller propagules, we induced apoptosis in the 14-transfer isolate by subculturing yeast in YPD supplemented with 40 mM acetate for 4 h (32). This increased the frequency of DHR-stained (apoptotic) cells from 0.2 to 2.7% and reduced propagule size to less than 30% that of parent clusters (Fig. 6*D*; $F_{1,20} = 6.07$, $P = 0.044$, Bonferroni-corrected preplanned contrast).

The selective benefits of apoptosis occur only in large snowflake phenotypes, as seen in the evolution of increased rates of apoptosis in faster-settling populations over the course of the experiment (Fig. 4*B*). As snowflake yeast evolved a twofold increase in size at reproduction over 14–60 transfers (Fig. 6*C*), propagule size

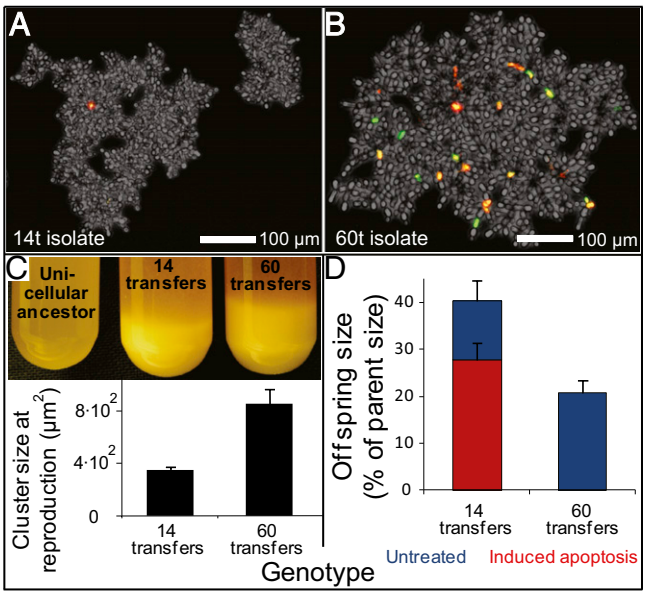

Fig. 6. High rates of apoptosis evolve, decreasing propagule size. (*A* and *B*) High rates of apoptosis evolve between transfers 14 and 60 in replicate population 1. Yeast were incubated with the red dead-cell stain propidium iodide (PI) and the apoptosis stain DHR. Cells in the early stages of apoptosis stain green; cells dying from apoptosis stain with both PI and DHR, appearing yellow/orange; and necrotic cells stain red. (*C*) By 60 transfers, snowflake yeast had evolved to settle more rapidly than the 14 transfer isolate. Shown are stationary-phase cultures allowed to settle on the bench for 10 min. This is due to an increase in the size of the cluster at reproduction. Shown are the averages of seven single-cluster overnight life-history analyses, per genotype. Error bars are the SEM. (*D*) Apoptosis decreases propagule size. The 60 transfer strain, which has evolved a larger size at reproduction (*C*) and increased rates of apoptosis relative to the 14 transfer strain (*A* and *B*), produces proportionally smaller propagules. Experimental induction of apoptosis in the 14 transfer strain reduced propagule size. Shown are the averages of eight (14 and 60 transfers, apoptosis not induced) and seven (14 transfers, apoptosis induced) single-cluster overnight life-history analyses. Error bars are SEM.

declined from 40 to 20% of parental size (Fig. 6*D*). Because clusters that make smaller propagules can make more of them, apoptosis by a subset of cells should be adaptive, allowing large clusters to allocate reproduction into a greater number of propagules than with the more symmetric division that occurs without apoptosis (Fig. 6*D*). Even though such propagules start smaller, their faster relative growth rates mean that most will grow large enough during the 24 h between transfers to survive gravitational selection.

Discussion

Although known transitions to complex multicellularity, with clearly differentiated cell types, occurred over millions of years (9, 33), we have shown that the first crucial steps in the transition from unicellularity to multicellularity can evolve remarkably quickly under appropriate selective conditions. Multicelled snowflake-phenotype yeast evolved in all 15 replicate populations, in two separate experiments, within 60 d of settling selection. All snowflake yeast formed clusters through postdivision adhesion, not aggregation. This method of growth ensures high relatedness among individual cells within the cluster, aligning the fitness of individual cells with their genetically identical kin within a cluster (6, 24). Aggregation through floc-type adhesion was not observed in any of our experiments, possibly because this method of growth is prone to within-group conflict (25). Choanoflagellates, the closest unicellular ancestor to animals, can form multicellular colonies through postdivision adhesion (34), raising the possibility that a similar step was instrumental in the evolution of animal multicellularity.

We observed adaptation of multicellular traits, indicating a shift in selection from individual cells to multicellular individuals. In response to selection for even more rapid settling, snowflake-phenotype yeast adapted through changes in their multicellular life history, increasing the length of the juvenile phase that precedes production of multicellular propagules. We also observed the evolution of division of labor within the cluster: most cells remain viable and reproduce, but a minority of cells become apoptotic. Apoptotic cells act as break points within multicellular clusters, allowing snowflake yeast to produce a greater number of propagules from a given number of cells. This is functionally analogous to germ-soma differentiation, where cells specialize into reproductive and nonreproductive tasks (35). These results demonstrate that multicellular traits readily evolve as a consequence of among-cluster selection.

Apoptosis is integral to development and somatic maintenance in extant metazoans (36). Apoptosis-like cellular suicide is also surprisingly widespread among unicellular organisms, including *S. cerevisiae* (29–31, 37), and was present in our ancestral unicellular strain. However, apoptosis rapidly evolved a new, co-opted function in our multicellular yeast with no obvious parallel in the unicellular ancestor. Similarly, the existence of apoptosis-like cellular suicide in the unicellular ancestors of metazoans (38) may be an important preadaptation, facilitating the evolution of complex multicellularity (39). Apoptotic cells, like nonreproductive somatic tissue, leave no direct descendants once they differentiate. Their frequency never evolved beyond 2% in any of our snowflake-phenotype yeast strains. This is consistent with the hypothesis that the earliest somatic tissue should constitute only a small percentage of the multicelled organism's biomass; otherwise, the fitness cost of nonreproductive tissue would outweigh the benefit of divided labor (21).

Our results are consistent with several observations on the tempo and mode of the evolution of multicellularity. Recent studies of volvocine multicellularity demonstrate that, contrary to some theoretical expectations (40), the evolution of multicellularity does not require extensive expansion of genomic complexity (41). The fossil record shows that long periods of stasis are often punctuated by bursts of rapid evolution (42), presumably due to shifts in selective conditions and dramatic evolutionary responses. Over the history of life, multicellularity has evolved repeatedly in unrelated phylogenetic groups (10). The potential for the evolution of multicellularity may be less constrained than is frequently postulated.

Materials and Methods

Methods for our main selection procedures, relative fitness assays, divergent selection experiment, cluster-level life-history analyses, and analysis of trade-offs between growth and settling rates are found in *SI Materials and Methods*. Methods for the experimental induction of apoptosis, quantification of apoptosis, determination that dead-cells are involved in propagule production and selfing sex experiments can also be found in *SI Materials and Methods*. Methods for preparation and analysis of fluorescent images are also in *SI Materials and Methods*.

ACKNOWLEDGMENTS. We thank Kristin Jacobsen, Mitch Hoverman, and Amanda Muehlbauer for laboratory assistance; Mark Sanders at the University of Minnesota Imaging Center for microscopy help; and Barry Williams for providing GFP-labeled Y55. We also thank Ruth Shaw, James Griesemer, Xiao Yi, Ed Hall, Tony Dean, Ken Waters, Joan Strassman, Igor Lourbel, Tim Cooper, Ricardo Azevedo, Matthew Herron, and Alan Love for helpful feedback. This work was supported by National Science Foundation Grants DEB-0918897 and DEB-1051115.

1. Maynard Smith J, Szathmáry E (1995) *The Major Transitions in Evolution* (Oxford University Press, New York).

2. Simpson C (2012) The evolutionary history of division of labour. *Proc Biol Sci* 279 (1726):116–121.

3. Kirk DL (2005) A twelve-step program for evolving multicellularity and a division of labor. *Bioessays* 27:299–310.
4. Merlo LMF, Pepper JW, Reid BJ, Maley CC (2006) Cancer as an evolutionary and ecological process. *Nat Rev Cancer* 6:924–935.
5. Ostrowski EA, Katoh M, Shaulsky G, Queller DC, Strassmann JE (2008) Kin discrimination increases with genetic distance in a social amoeba. *PLoS Biol* 6:e287.
6. Grosberg RK, Strathmann RR (1998) One cell, two cell, red cell, blue cell: The persistence of a unicellular stage in multicellular life histories. *Trends Ecol Evol* 13(3): 112–116.
7. Campisi J, Kim SH, Lim CS, Rubio M (2001) Cellular senescence, cancer and aging: The telomere connection. *Exp Gerontol* 36:1619–1637.
8. Leroi AM, Koufopanou V, Burt A (2003) Cancer selection. *Nat Rev Cancer* 3:226–231.
9. Herron MD, Hackett JD, Aylward FO, Michod RE (2009) Triassic origin and early radiation of multicellular volvocine algae. *Proc Natl Acad Sci USA* 106:3254–3258.
10. Grosberg RK, Strathmann RR (2007) The evolution of multicellularity: A minor major transition? *Annu Rev Ecol Evol Syst* 38:621–654.
11. Herron MD, Michod RE (2008) Evolution of complexity in the volvocine algae: Transitions in individuality through Darwin's eye. *Evolution* 62:436–451.
12. Willensdorfer M (2008) Organism size promotes the evolution of specialized cells in multicellular digital organisms. *J Evol Biol* 21(1):104–110.
13. Bonner JT (1998) The origins of multicellularity. *Integr Biol Issues News Rev* 1(1):27–36.
14. Pfeiffer T, Bonhoeffer S (2003) An evolutionary scenario for the transition to undifferentiated multicellularity. *Proc Natl Acad Sci USA* 100:1095–1098.
15. Damuth J, Heisler IL (1988) Alternative formulations of multilevel selection. *Biol Philos* 3:407–430.
16. Boraas ME, Seale DB, Boxhorn JE (1998) Phagotrophy by a flagellate selects for colonial prey: A possible origin of multicellularity. *Evol Ecol* 12(2):153–164.
17. Michod R (2005) On the transfer of fitness from the cell to the multicellular organism. *Biol Philos* 20:967–987.
18. Koschwanez JH, Foster KR, Murray AW (2011) Sucrose utilization in budding yeast as a model for the origin of undifferentiated multicellularity. *PLoS Biol* 9:e1001122.
19. Michod RE, Viossat Y, Solari CA, Hurand M, Nedelcu AM (2006) Life-history evolution and the origin of multicellularity. *J Theor Biol* 239:257–272.
20. Diggle SP, Griffin AS, Campbell GS, West SA (2007) Cooperation and conflict in quorum-sensing bacterial populations. *Nature* 450:411–414.
21. Willensdorfer M (2009) On the evolution of differentiated multicellularity. *Evolution* 63:306–323.
22. Bonner JT (2003) On the origin of differentiation. *J Biosci* 28:523–528.
23. Queller DC, Strassmann JE (2009) Beyond society: The evolution of organismality. *Philos Trans R Soc Lond B Biol Sci* 364:3143–3155.
24. Hamilton WD (1964) The genetical evolution of social behaviour. I. *J Theor Biol* 7: 1–16.
25. Smukalla S, et al. (2008) FLO1 is a variable green beard gene that drives biofilm-like cooperation in budding yeast. *Cell* 135:726–737.
26. Taheri N, Köhler T, Braus GH, Mösch HU (2000) Asymmetrically localized Bud8p and Bud9p proteins control yeast cell polarity and development. *EMBO J* 19:6686–6696.
27. Buss LW (1987) *The Evolution of Individuality* (Princeton University Press, Princeton, NJ).
28. Rainey PB, Kerr B (2010) Cheats as first propagules: A new hypothesis for the evolution of individuality during the transition from single cells to multicellularity. *Bioessays* 32(10):872–880.
29. Rodriguez-Menocal L, D'Urso G (2004) Programmed cell death in fission yeast. *FEM Yeast Res* 5(2):111–117.
30. Madeo F, et al. (1999) Oxygen stress: A regulator of apoptosis in yeast. *J Cell Biol* 145: 757–767.
31. Carmona-Gutierrez D, et al. (2010) Apoptosis in yeast: Triggers, pathways, subroutines. *Cell Death Differ* 17:763–773.
32. Ludovico P, Sousa MJ, Silva MT, Leão C, Côrte-Real M (2001) Saccharomyces cerevisiae commits to a programmed cell death process in response to acetic acid. *Microbiology* 147:2409–2415.
33. Srivastava M, et al. (2010) The Amphimedon queenslandica genome and the evolution of animal complexity. *Nature* 466:720–726.
34. Fairclough SR, Dayel MJ, King N (2010) Multicellular development in a choanoflagellate. *Curr Biol* 20:R875–R876.
35. Michod RE, Nedelcu AM (2003) On the reorganization of fitness during evolutionary transitions in individuality. *Integr Comp Biol* 43(1):64–73.
36. Meier P, Finch A, Evan G (2000) Apoptosis in development. *Nature* 407:796–801.
37. Nedelcu AM, Driscoll WW, Durand PM, Herron MD, Rashidi A (2011) On the paradigm of altruistic suicide in the unicellular world. *Evolution* 65(1):3–20.
38. Nedelcu AM (2009) Comparative genomics of phylogenetically diverse unicellular eukaryotes provide new insights into the genetic basis for the evolution of the programmed cell death machinery. *J Mol Evol* 68:256–268.
39. Huettenbrenner S, et al. (2003) The evolution of cell death programs as prerequisites of multicellularity. *Mutat Res* 543:235–249.
40. Lynch M (2007) The frailty of adaptive hypotheses for the origins of organismal complexity. *Proc Natl Acad Sci USA* 104(Suppl 1):8597–8604.
41. Prochnik SE, et al. (2010) Genomic analysis of organismal complexity in the multicellular green alga Volvox carteri. *Science* 329:223–226.
42. Eldredge N, et al. (2005) The dynamics of evolutionary stasis. *Paleobiology* 31(sp5): 133–145.

Supporting Information

Ratcliff et al. 10.1073/pnas.1115323109

SI Materials and Methods

Gravitational Selection, Experiment 1. Ten replicate populations of initially genetically uniform dioloid *Saccharomyces cerevisiae* strain Y55 were grown in 10-mL aliquots of Yeast Peptone Dextrose (YPD; per liter: 10 g yeast extract, 20 g peptone, 20 g dextrose, pH 5.8) in 25- × 150-mm glass culture tubes at 30 °C, shaking at 250 × *g*. Every 24 h, the entire population was transferred to a 16- × 150-mm sterile glass tube and allowed to settle on the bench for 45 min, and the bottom 100 μL was transferred to the next 25-mm culture tube containing fresh rich media. After 7 d, the transfer step was made more efficient: 1.5 mL of each culture was removed and centrifuged at 100 × *g* for 10 s, and then the bottom 100 μL was transferred to the next 25-mm culture tube containing fresh media.

Gravitational Selection, Experiment 2. To examine the relative fitness of snowflake-phenotype yeast vs. unicellular yeast, we repeated experiment 1 (using 100 × *g* centrifugations to impose settling selection) on five replicate populations of the ancestral strain of Y55. In a parallel treatment, five replicate populations were transferred without gravitational settling. For both this and the previous experiment, a single, representative isolate was obtained from each replicate population after 60 transfers by picking and restreaking a single colony on YPD petri plates three times.

Relative Fitness of Unicellular vs. Multicellular Genotypes. Five snowflake-phenotype or unicellular single-strain isolates (experiment 2, above) were grown for 24 h in YPD and then diluted by a factor of 1/200 into 10 mL YPD (in 25- × 150-mm tubes) along with a common competitor: GFP-labeled unicellular Y55, also diluted by 1/200 from an overnight culture. After 24 h of growth, 100 μL from each tube was transferred to fresh media, either with or without selection imposed by centrifugation (100 × *g* for 10 s), and grown for another 24 h. The population size of both test and reference strains was determined at time 0 and after 48 h growth by imaging five predetermined fields of view in a hemocytometer for each replicate population. Image analysis in ImageJ was used to count the number of clusters with more than seven cells in brightfield illumination, and GFP-labeled unicells were counted by fluorescence microscopy. We determined the number of evolved unicellular cells by subtracting the number of GFP-marked cells from a count of the total number of unicells in the field of view. Malthusian growth parameters for each test strain relative to the common competitor were determined following the method of Lenski et al. (1). For this assay, we measured the fold increase in individuals (either multicellular clusters or individual cells for the snowflake and unicellular genotypes, respectively). Our a priori hypotheses were that clustering would increase settling rate, and thus fitness, when transferred with gravitational selection, but would decrease the rate at which nutrients and oxygen are absorbed by interior cells, resulting in reduced fitness in the absence of gravitational selection. Significance was thus tested with one-sided *t* tests.

Divergent Selection for Settling Rate. A single population of snowflake-phenotype yeast (from experiment 1, replicate population 1, 30 transfers) was put under divergent selection for settling rate. Cell culture was performed as above. Three replicate populations per treatment were exposed to strong, medium, or weak gravitational selection for settling rate by subculturing 1.5 mL into a microcentrifuge tube and allowing this to settle on the bench for 5, 15, or 25 min, respectively. As in the other experiments, the lower 100 μL was then transferred to fresh media. This was carried out for 35 daily transfers. Settling rate was measured by placing 1 mL of stationary-phase cells in a 1.5-mL centrifuge tube, allowing the yeast to settle at 1 × *g* for 7 min and then fractionating the upper 700 μL and lower 300 μL. These subsamples were pelleted and double-washed in deionized (DI) water, excess water was removed, and the pellet was air-dried at 50 °C for 2 d. Settling rate was determined by the percentage of total biomass in each fraction.

Cluster-Level Life-History Analysis. Individual clusters were inoculated into 0.5-μL droplets of YPD and placed on the bottom of an eight-well Lab-Tek II chambered coverglass slide. Ten microliters of water was placed in each corner of the chamber, and clear tape was placed over the chamber top to keep the microdroplet from drying out. These clusters were then imaged on an Olympus IX70 inverted microscope. Using the 10× objective, brightfield illumination (set extremely low to avoid overheating the yeast), and a 1-s acquisition time, images were captured every minute with a SPOT 4MP camera in overnight time courses. Cluster size at reproduction was determined by manually outlining the perimeter of the reproducing cluster (one frame before a propagule was produced) in ImageJ and then measuring the outlined area. Propagule size was also determined by manual annotation.

Trade-Off Between Growth and Settling Rates. We chose 5/10 of the replicate populations from our first experiment that captured the range of cluster sizes evolved after 60 transfers. A representative genotype was isolated from each replicate (single colony selection, repeated three times serially) for the first time point at which we detected snowflake yeast and from 60 transfers. For the settling rate assay, five replicates of each genotype were conditioned by 24 h growth in 10 mL YPD, transferred to fresh media with selection for settling (100 × *g* for 10 s), and incubated at 30 °C for 24 h. Settling rate was determined as described in the divergent selection experiment above. Growth rate was determined by growing five replicates of each genotype for 24 h, diluting 1:100 without gravitational selection into 10 mL of fresh YPD (thereby transferring similar biomass), and then allowing yeast to grow for 12 h. From these actively growing cells, 100 μL was removed and added to 900 μL fresh YPD in 15-mL centrifuge tubes. These cells were grown for 4 h at 30 °C, and then the fold increase in biomass was determined by pellet washing and drying as previously described.

Quantification of Apoptosis. Apoptosis was measured by dihydrorhodamine 123 (DHR) staining of reactive oxygen species (2–4). Following the procedure of Madeo et al. (3), we stained cells with 1:100 of DHR stock solution (2.5 mg/mL in ethanol) for 2 h in the dark; cells were double-washed in sterile DI water and imaged microscopically. Before staining, yeast were conditioned by 24 h growth in YPD, followed by a 1:100 dilution (without gravitational selection) into fresh YPD where they were incubated for 12 h. Clusters were flattened into two dimensions by placing 5 μL of cell suspension between a standard slide and a 22- × 22-mm coverslip. Sample drying was minimized by sealing coverslip edges with clear nail polish. The frequency of apoptotic cells was measured for three independent replicates of each genotype on five fields of view per replicate. For each field of view, total cluster area was measured with brightfield microscopy, and DHR-stained cell area was measured by fluorescence microscopy for the same cells. In each case, background pixels were removed by thresholding; threshold values were kept as consistent as possible with small adjustments made for minor variation in background intensity.

Fluorescence Overlay. Fluorescence overlay was done in ImageJ with the "merge channels" command. The background brightfield, phase contrast, or differential interference contrast image was set to gray, propidium iodide (PI) to red, and DHR to green. To make fluorescence more visible in merged images, PI and DHR brightness was increased. Brightness was increased identically for all samples of a particular fluorophore in each experiment.

Experimental Induction of Apoptosis. Apoptosis was induced in snowflake yeast from replicate 1 at 14 transfers, a strain with wild-type levels of apoptosis. Following the proceedure of Ludovico et al. (5), we incubated stationary-phase snowflake yeast in YPD supplented with 40 mM acetate at pH 3.0 for 4 h and then washed cells centrifugally and resuspended them in standard YPD.

Dead Cell Involvement in Propagule Production. To determine if dead cells frequently serve as a break point for propagule production, we examined 17 randomly selected propagules that contained at least one dead cell. Propagules were obtained by diluting stationary-phase replicate 1, 60 transfer snowflake yeast 1:100 into fresh YPD and culturing for 4 h. Propagules were distinguished from parental clusters by size. For each, the center cell (the site of propagule separation) was determined as described in Fig. S3. Viability of this center cell was determined by PI staining. Statistical significance was assessed with a binomial probability test. The overall frequency of dead cells (live/dead cells were counted manually for all clusters) was used as our null expectation that the center cell would be dead.

Selfing Snowflake Yeast. To determine if apoptosis and cluster size are genetically independent traits, we selfed a large-cluster-forming, high-apoptosis strain. This strain evolved in the 5-min settling treatment of the divergent selection experiment. To induce sex, we streaked cells out onto sporulation agar (per liter: 20 g potasium acetate, 2.2 g yeast extract, 870 mg synthetic complete amino acid mix, 0.5 g glucose) and incubated the cells at 30 °C for 4 d. Individual spores were obtained by enzymatically digesting tetrads in 1,000 units of lyticase and 2% β-glucuronidase/arylsulfatase (Roche) for 1 h at 28 °C and then by vortexing tetrads with 50% (vol/vol) 0.1-mm glass beads for 60 s. Complete digestion of tetrads was confirmed by microscopy. Individual spores were plated on YPD agar, and one isolate was obtained from one colony by three rounds of streaking and single-colony isolation. Selfing a single spore was possible because the ancestral strain Y55 switches mating types. All isolates obtained were diploid and are presumed homozygous at all loci, excepting the *MAT* loci.

1. Lenski RE, Rose MR, Simpson SC, Tadler SC (1991) Long-term experimental evolution in escherichia coli. I. Adaptation and divergence during 2,000 generations. *Am Nat* 138:1315–1341.
2. Rodriguez-Menocal L, D'Urso G (2004) Programmed cell death in fission yeast. *FEM Yeast Res* 5(2):111–117.
3. Madeo F, et al. (1999) Oxygen stress: A regulator of apoptosis in yeast. *J Cell Biol* 145: 757–767.
4. Carmona-Gutierrez D, et al. (2010) Apoptosis in yeast: Triggers, pathways, subroutines. *Cell Death Differ* 17:763–773.
5. Ludovico P, Sousa MJ, Silva MT, Leão C, Côrte-Real M (2001) Saccharomyces cerevisiae commits to a programmed cell death process in response to acetic acid. *Microbiology* 147:2409–2415.

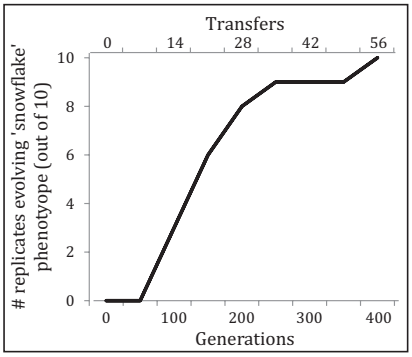

Fig. S1. Rapid evolution of snowflake-phenotype yeast. Snowflake phenotypes arose rapidly in response to strong selection for rapid settling. Plotted is the number of replicates with detectable snowflake phenotype (determined by plating on YPD agar and isolation of nonsmooth colony morphs and confirmed by microscopy) as a function of the number of transfers (or estimated generations) in our first 10-replicate selection experiment.

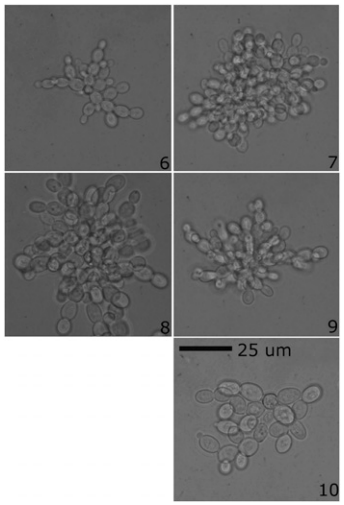

Fig. S2. Representative snowflake-phenotype yeast from replicate populations 6–10, isolated after 60 transfers (see Fig. 1 for replicate populations 1–5).

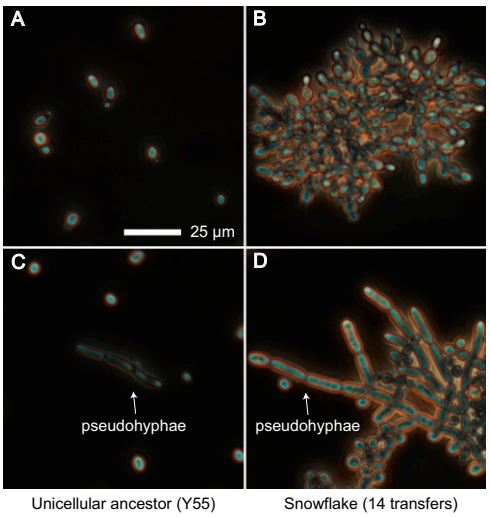

Fig. S3. Clustering occurs independently of pseudohyphal growth. *S. cerevisiae* has previously been shown to form clusters through pseudohyphal growth (1). Pseudohyphal cells are characterized by cellular elongation and are expressed on solid media in response to nitrogen starvation (2). (*A* and *B*) When grown in liquid YPD overnight, both the ancestral unicellular strain and snowflake-phenotype yeast exhibit normal, oval-cell morphology. To determine if pseudohyphae can be induced in the unicellular ancestor and snowflake yeast from replicate population 1, 14 transfers, we starved yeast by culturing them on solid YPD media for 5 d. Pseudohyphae were readily observed in both strains (*C* and *D*). We conclude that the snowflake phenotype is not the result of a mutation that made previously inducible pseudohyphal cell morphology constitutive.

1. Van de Velde S, Thevelein JM (2008) Cyclic AMP-protein kinase A and Snf1 signaling mechanisms underlie the superior potency of sucrose for induction of filamentation in Saccharomyces cerevisiae. *Eukaryot Cell* 7:286–293.
2. Gimeno CJ, Ljungdahl PO, Styles CA, Fink GR (1992) Unipolar cell divisions in the yeast S. cerevisiae lead to filamentous growth: Regulation by starvation and RAS. *Cell* 68:1077–1090.

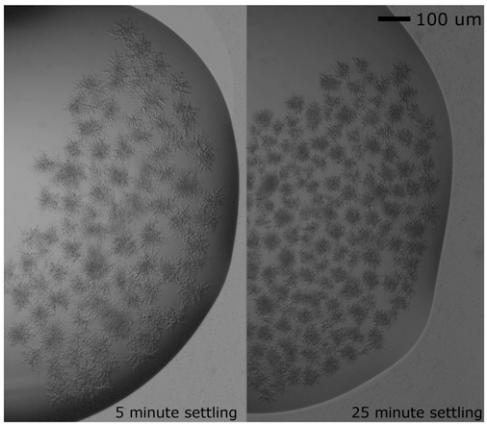

Fig. S4. Size of the multicellular cluster is approximately determinate. A single cluster was inoculated into a 0.5-μL droplet of YPD and grown for 16 h; shown are the resulting populations. The similar size distribution of the resulting offspring clusters (within each population), despite generational differences, demonstrates that the size of the multicellular cluster is approximately determinate. Cells in large clusters do not stop dividing. Instead, ongoing cell growth results in propagule production. (*Left*) A randomly selected isolate from the 5-min settling treatment. (*Right*) A randomly selected isolate from the 25-min settling treatment from the divergent selection experiment (Fig. 3).

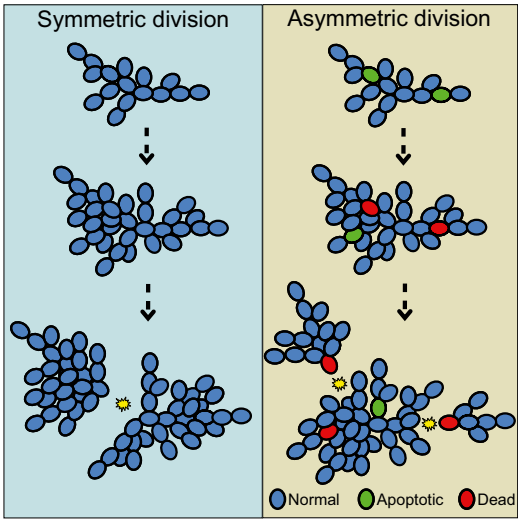

Fig. S5. Proposed role of apoptosis in reducing propagule size. Cell death through apoptosis generates "weak links" between chains of cells in a cluster. As cells within the cluster divide, they grow into one another, putting a strain on the connection between cells. Dead cells break more easily, resulting in earlier cell separation and the production of smaller propagules.

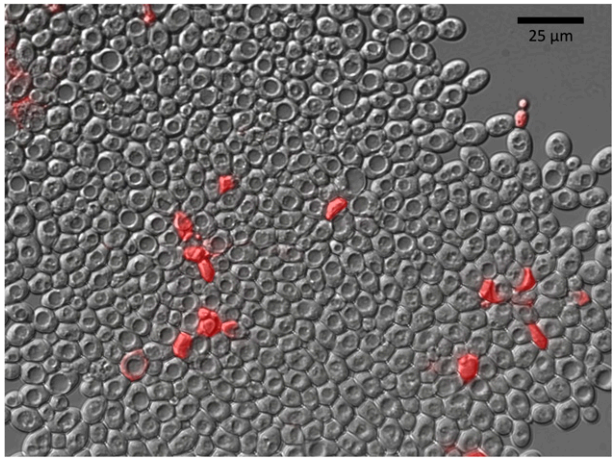

Fig. S6. Dead cells exhibit aberrant morphology. Snowflake-phenotype yeast (drawn from replicate population 1, day 60, of our first evolution experiment) were grown for 24 h in YPD, stained with propodium iodide (PI), flattened between a coverslip and slide, and imaged on a Nikon E800 microscope. Shown is a differential interference contrast background image with PI fluorescence overlay (42% opacity).

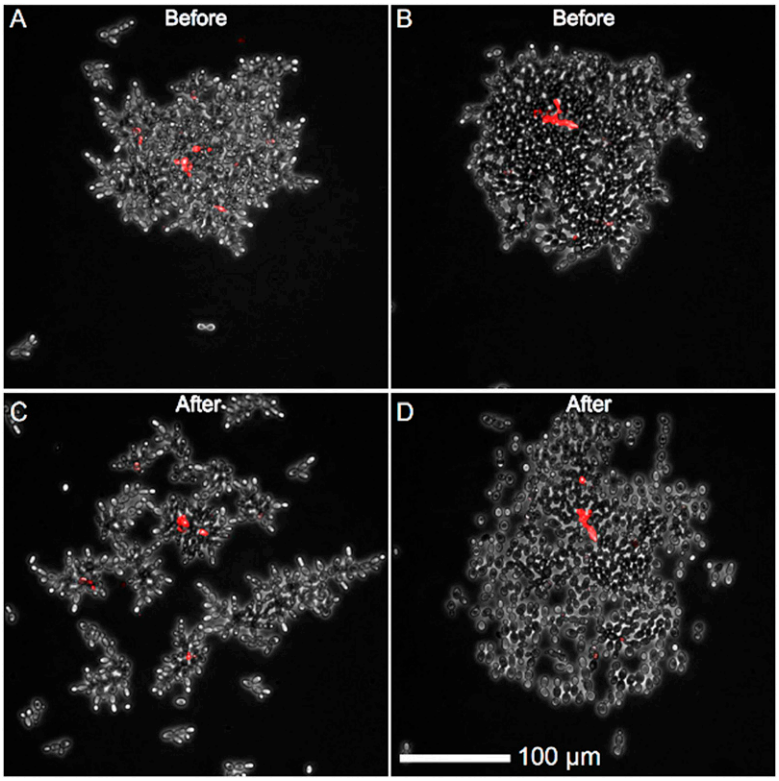

Fig. S7. Cell separation does not cause cell death. To determine if cell separation, the process that produces propagules, causes cell death, we manually fragmented snowflake yeast from replicate population 1, 60 transfers. Yeast were grown for 24 h under standard culture conditions, diluted 1:10 into water, and stained with propidium iodide for 5 min. Five microliters of cells and staining solution was placed on a slide and covered with a 22- × 22-mm coverslip. Clusters were imaged immediately, and then the coverslip was moved in a small circular motion to break the cluster apart. After 5 min, fragmented clusters were reimaged. Regardless of whether snowflake yeast were broken into smaller clusters (*A* and *C*) or into mostly pairs of cells (*B* and *D*), no cell death was induced.

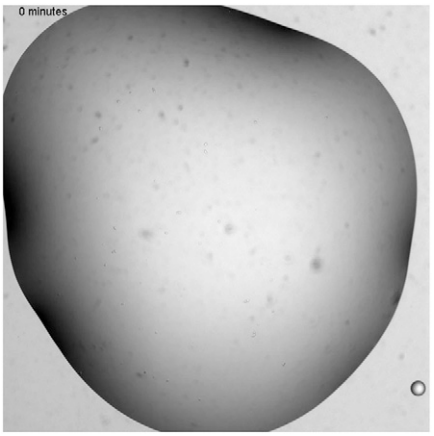

Movie S1. Single cells of snowflake-phenotype yeast regenerate new snowflake-phenotype clusters. Snowflake-phenotype clusters (drawn from replicate population 1, day 60, of our first evolution experiment) were broken down into unicells by digestion with lyticase (500 units/mL in H_2O, 45-min digestion at 22 °C, vigorous vortexing for 5 min). These cells were then diluted 300-fold and grown in 0.5 μL YPD. Time-lapse microscopy was performed at 100× magnification, with images taken every minute for 760 min. Note that these are all "juveniles"; no multicellular propagule production by any clusters was observed during the experiment.

Movie S1

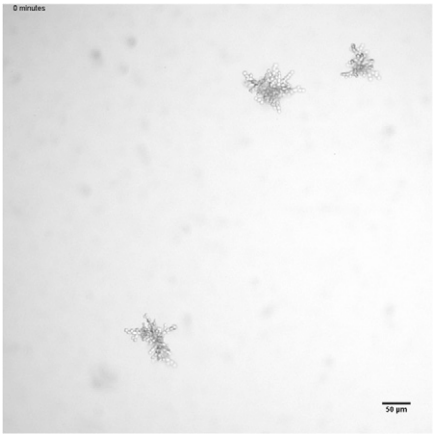

Movie S2. Growth of snowflake-phenotype yeast. Snowflake-phenotype clusters (same genotype as in Movie S1) were diluted by 300-fold and grown in 0.5 μL YPD. Time-lapse microscopy was performed at 100× magnification, with images taken every minute for 500 min.

Movie S2

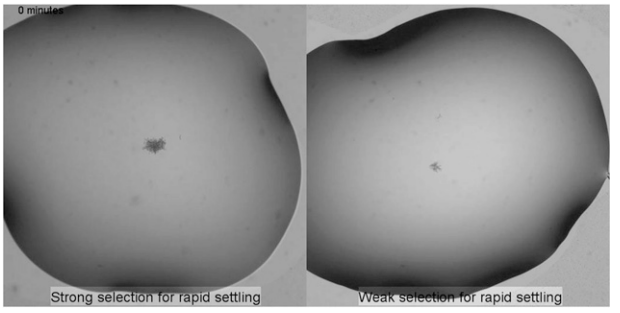

Movie S3. Time-lapse microscopy of derived rapid settling (*Left*) and slow settling (*Right*) genotypes isolated from 5- and 25-min settling regimes, respectively. Cultures were grown for 24 h, diluted 300-fold, and grown in 0.5 μL YPD. Time-lapse microscopy was performed with images taken every minute for 600 min.

Movie S3

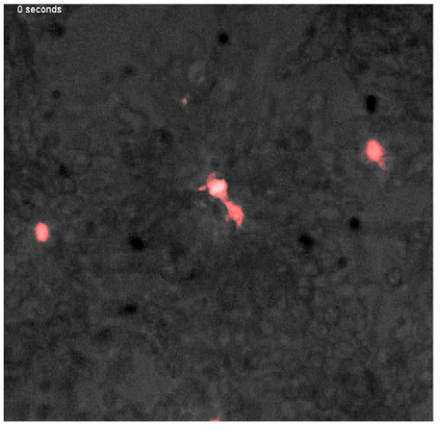

Movie S4. Cluster fragmentation occurring between a pair of dead cells. This video captures production of a propagule by fragmentation. Cell separation occurs at the connection between two cells that stain with propidium iodide (PI). Snowflake yeast (replicate population 1, 60 transfers) were grown in 100 μL of YPD with 1% PI stock solution in eight-well Lab-Tek II chambered coverglass slides. Snowflake yeast were illuminated with low-intensity halogen light and PI excited by green light (dimmed with a 50% opacity neutral density filter); images were captured every 5 s at 400× magnification. To compose the movie, individual frames (RGB Imaging) were decomposed into their component colors; the red component was then thresholded to remove cells that were not emitting PI fluorescence. The original images were converted to 8 bit, and the thresholded images containing PI fluorescence data were entered as the red channel using the "merge channels" command in ImageJ.

Movie S4